

HOSTED BY



Contents lists available at ScienceDirect

# Atmospheric Pollution Research

journal homepage: <http://www.journals.elsevier.com/locate/apr>

Original article

## Impact of environmental variables on the reduction of nitric acid by proxies for volatile organic compounds emitted by motor vehicles



Y.J. Leong<sup>a,\*</sup>, A.P. Rutter<sup>a,b</sup>, H.Y. Wong<sup>a,c</sup>, C.V. Gutierrez<sup>a</sup>, M. Junaid<sup>a</sup>, E. Scheuer<sup>d</sup>,  
L. Gong<sup>a,e</sup>, R. Lewicki<sup>f,g</sup>, J.E. Dibb<sup>d</sup>, F.K. Tittel<sup>f</sup>, R.J. Griffin<sup>a</sup>

<sup>a</sup> Rice University, Civil and Environmental Engineering, 6100 Main Street MS-519, Houston, TX 77005, United States

<sup>b</sup> (Current) Collaborative Sciences Division, S.C. Johnson, Inc., 1525 Howe St., Racine, WI 53403, United States

<sup>c</sup> (Current) Behn Meyer Group Malaysia, 5, Jalan TP2 Sime UEP Industrial Park, Subang Jaya, Selangor 47600, Malaysia

<sup>d</sup> University of New Hampshire, Earth Systems Research Center, Morse Hall, Durham, NH 03824, United States

<sup>e</sup> (Current) Monitoring and Laboratory Division, California Air Resources Board, 1900 14th Street, Sacramento, CA 95811, United States

<sup>f</sup> Department of Electrical and Computer Engineering, Rice University, 6100 Main Street, MS 366, Houston, TX 77005, United States

<sup>g</sup> (Current) Sentinel Photonics, 45 Wall Street, Princeton, NJ 08540, United States

### ARTICLE INFO

#### Article history:

Received 8 June 2015

Received in revised form

4 September 2015

Accepted 5 September 2015

Available online 21 October 2015

#### Keywords:

Nitrous acid

Nitric acid

Volatile organic compounds

Flow tube

Reduction-oxidation

### ABSTRACT

Recent work has identified nitric acid (HNO<sub>3</sub>) as a potential precursor of nitrous acid (HONO), which is an important source of oxidants that regulate ozone and particulate pollution. Recent work in our laboratory has indicated that the reduction of HNO<sub>3</sub> to HONO can occur homogeneously in the presence of surrogates for volatile organic compounds (VOCs) emitted by motor vehicles. This study focuses on the impact of environmental variables on the rate of formation of HONO in this process. The observed base case (25.0 °C and ~20.0% relative humidity (RH)) HONO formation rate was 0.54 ± 0.09 ppb h<sup>-1</sup>, values comparable to enhancements observed in HONO during morning rush hour in Houston, TX. The rate was enhanced at lower temperatures of ~20.0 °C, but the rate remained statistically similar (1σ) for experiments conducted at temperatures of 25 °C, 30 °C, and 35 °C. The assumption that multiple reactive components of the VOC mixture react with HNO<sub>3</sub> is supported by this observation, and the relative importance of each reactive species in the reaction may vary with temperature. The enhanced rate at lower temperatures could make the proposed reaction mechanism more important at night. The formation rate of HONO does not change substantially when initial HNO<sub>3</sub> concentration is varied between 400 and 4600 ppt, suggesting that the concentration of reactive VOCs was the limiting factor. The reduction of HNO<sub>3</sub> to HONO appears not to occur heterogeneously on the aerosol surfaces tested. The presence of ~120 ppb of ammonia has no observable impact on the reaction. However, it is likely that UV irradiation (λ = 350 nm) decreases the formation rate of HONO either by consuming the reactive VOCs involved or by directly interfering with the reaction. The “renoxification” of less reactive HNO<sub>3</sub> to more reactive HONO has significant implications for daytime ozone and particulate pollution.

Copyright © 2015 Turkish National Committee for Air Pollution Research and Control. Production and hosting by Elsevier B.V. All rights reserved.

### 1. Introduction

Nitrous acid (HONO) is an important trace gas in the regional and global troposphere. It can have significant air quality

implications due to its photolysis, yielding nitrogen oxide (NO) and the hydroxyl radical (OH) (Atkinson, 2000):



The OH radical serves as a strong oxidant in the atmosphere and is partly responsible for the chemical processes that lead to the formation of tropospheric ozone (O<sub>3</sub>) (Finlayson-Pitts and Pitts, 1997) and secondary particulate matter (PM) (Kanakidou et al., 2005). With nitrogen dioxide (NO<sub>2</sub>), NO contributes to total nitrogen oxide (NO<sub>x</sub>) levels. The potential of a regional air mass to

\* Corresponding author. Tel.: +1 713 348 3036; fax: +1 713 348 5268.

E-mail address: [yu.jun.leong@gmail.com](mailto:yu.jun.leong@gmail.com) (Y.J. Leong).

Peer review under responsibility of Turkish National Committee for Air Pollution Research and Control.

produce O<sub>3</sub> depends strongly on the relative abundance of volatile organic compounds (VOCs) and NO<sub>x</sub>. Because HONO influences NO<sub>x</sub> levels, O<sub>3</sub> pollution levels are highly sensitive to HONO levels under particular conditions (Harris et al., 1982; Lei et al., 2004; Carter and Seinfeld, 2012). Harris et al. (1982) observed increases in O<sub>3</sub> dosages up to a factor of 3 when 10 ppb of HONO is included in model simulations. Using a three-dimensional chemical transport model, Lei et al. (2004) estimated up to 12 ppb enhancements in O<sub>3</sub> levels in Houston, TX, due to a proposed heterogeneous source of HONO. Zero-dimensional model simulations of O<sub>3</sub> formation episodes in the Upper Green River Basin in Wyoming during winter predicted strong O<sub>3</sub> sensitivity to HONO levels (Carter and Seinfeld, 2012).

Nitrous acid mixing ratios observed at various urban sites range from 0.4 to 8.0 ppb at night and 100–300 ppt during the day (Harris et al., 1982; Harrison et al., 1996; Kleffmann, 2007; Wong et al., 2011; Indarto, 2012), while concentrations at rural sites were 10–200 ppt (Cape et al., 1992; Zhou et al., 2002, 2011). A known source of HONO during daytime in polluted environments is the reaction between OH and NO (Atkinson, 2000):



Nitrous acid builds up overnight from (R2) (when OH and NO persist without sunlight) and other sources and photolyzes in the morning, causing a spike in OH and NO<sub>x</sub>, resulting in accelerated O<sub>3</sub> production (Harris et al., 1982). Nitrous acid sources other than (R2) are thus highly important due to their potential to contribute to both daytime and nighttime HONO levels. Modeling studies have concluded that HONO sources are still missing from current hydrogen oxide (HO<sub>x</sub>) and NO<sub>x</sub> chemistry models, resulting in the underprediction of HONO or O<sub>3</sub> levels (Grannas et al., 2007; Wong et al., 2011; Carter and Seinfeld, 2012).

A number of recent studies have documented possible sources of HONO from HNO<sub>3</sub> or NO<sub>2</sub>. Kleffmann (2007) proposed several formation mechanisms: heterogeneously on surfaces treated with HNO<sub>3</sub>, from the reduction of NO<sub>2</sub> on photosensitized organic surfaces, and via photolysis of ortho-substituted nitroaromatics. Similarly, photolytic conversion of NO<sub>2</sub> to HONO on polycyclic aromatic hydrocarbon films was observed by Cazoir et al. (2014). Grannas et al. (2007) summarized several HONO formation mechanisms in a snowpack. In urban New Zealand, Reisinger (2000) observed a good correlation between HONO/NO<sub>2</sub> (a metric for the relative abundance of HONO) and aerosol surface density, indicating a heterogeneous HONO source. Nitrous acid forms on the surface of soot particles from NO<sub>2</sub>, but the reaction is not considered a major contributor to HONO under typical ambient conditions (Ammann et al., 1998; Kalberer et al., 1999). Kirchstetter et al. (1996) measured vehicular emissions of HONO in the Caldecott Tunnel, but the observed HONO/NO<sub>2</sub> ratios were much lower than the nighttime values measured under ambient conditions. In addition, recent airborne measurements coupled with zero-dimensional model simulations inferred a strong gas-phase source within the residual layer with formation rates that scaled with HONO photolysis rates (Li et al., 2014). The authors argued that this unknown source could dominate overall HONO production in the planetary boundary layer, exceeding surface HONO sources. The proposed ultraviolet (UV)-dependent HONO source was likely internal (from the reaction of NO<sub>x</sub> and/or HO<sub>x</sub>). Liu et al. (2014) proposed a substantial heterogeneous HONO source from the hydrolytic disproportionation of NO<sub>2</sub> on aerosol to help explain missing daytime HONO sources in China. Flow tube studies by VandenBoer et al. (2015) suggested a nighttime soil sink of HONO, leading to daytime acid displacement and release of HONO. A review of the current state of the science for HONO can be found in Spataro and Ianniello (2014).

In September 2006 in Houston, TX, Ziemba et al. (2010) observed HNO<sub>3</sub> depletion concurrent with increases in HONO concentrations and aerosol surface area dominated by a proxy for primary organic aerosol (POA). The authors hypothesized a heterogeneous reaction between HNO<sub>3</sub> and POA to form HONO, which supports the findings from previous studies that document the heterogeneous reduction of HNO<sub>3</sub> (Zhou et al., 2002; Rivera-Figueroa et al., 2003; Zhou et al., 2003, 2011).

In an effort to better understand the phenomenon observed by Ziemba et al. (2010), Rutter et al. (2014) performed a series of flow tube experiments in which gaseous HNO<sub>3</sub> was observed to be reduced homogeneously to HONO by VOCs representative of those emitted from motor vehicles via the hypothesized reaction:



The reported formation rate of HONO was  $0.3 \pm 0.1$  ppb h<sup>-1</sup> under a defined base case of 25.0 °C and RH of ~20%. The HONO formation rates decreased with increasing RH. Increased surface area in the flow-tube (Teflon® Raschig rings and/or a surrogate for vehicular POA) had no impact on HONO formation. The experiments described here used a slightly modified and improved version of the flow-tube system of Rutter et al. (2014) to further characterize this HONO formation reaction by varying temperatures and HNO<sub>3</sub> concentrations, irradiating, or adding ammonia (NH<sub>3</sub>) or mineral dust surrogates. These experiments are designed to improve our understanding of the importance of the proposed HONO formation reaction under varying ambient conditions and to assess its potential to enhance HONO levels in the atmosphere.

## 2. Experimental

### 2.1. General information

The flow-tube system used in this study is described by Rutter et al. (2014), with improvements and additional instrumentation described below. Briefly, HNO<sub>3</sub> gas and VOCs from a specific blend of vehicle engine oil (Supporting material, Table S1) were introduced into a quartz flow reactor, which is located in a temperature-controlled chamber. Nitric acid was generated from a permeation device (Dynacal, VICI Metronics, Poulosbo, WA), and engine oil particles along with VOCs were introduced using a TSI 3076 atomizer (Shoreview, MN) with a Teflon® filter in-line when the particles were not desired. A combustion VOC surrogate was not used for this study as the original intent was to use reduced organics from motor oil (Rutter et al., 2014); this avoids possible HONO artifacts from combustion exhaust (Kirchstetter et al., 1996). A recent tunnel study showed that a large portion of vehicular POA is similar in composition to unburned motor oil (Worton et al., 2014). The VOCs used in this study were intended to serve as surrogates for VOCs produced from the volatilization of vehicular POA under ambient conditions. The outflow from the flow-tube was sampled by a refurbished on-line mist chamber-ion chromatograph (MC/IC) system (Rutter et al., 2014) to obtain 10-min HONO and HNO<sub>3</sub> concentrations. This measurement technique has been tested and characterized extensively (Talbot et al., 1990; Dibb et al., 1994, 1998, 2002) and showed good comparison with Differential Optical Absorption Spectroscopy (Stutz et al., 2010). A new quartz flow-tube with dimensions identical to those of the reactor in Rutter et al. (2014) was used and was passivated by a non-reactive halocarbon wax coating to minimize wall reactions. Instrumentation used to measure temperature, RH, and particle number concentration were outlined in Rutter et al. (2014). The instrumentation for measuring NH<sub>3</sub> is described below.

In this study, the base case experiments were conducted at a temperature of 25 °C and a RH of ~20% while maintaining a mean HNO<sub>3</sub> concentration of 2.4 ppb and a constant level of VOCs in the flow-tube reactor. For each experiment, the flow-tube reactor was allowed to equilibrate at the desired conditions (concentrations of HNO<sub>3</sub> and VOCs, temperature, RH, and other variables). The formation rates of HONO ( $f_{HONO}$ , ppb h<sup>-1</sup>) were calculated using the step change in HONO concentrations when VOCs were removed:

$$f_{HONO} = ([HONO]_t - [HONO]_0) / t_{res} \quad (1)$$

where  $[HONO]_t$  (in ppb) was the average steady-state HONO concentration measured when VOCs were present to react with HNO<sub>3</sub>,  $[HONO]_0$  was measured after VOCs were removed and only HNO<sub>3</sub> was present, and  $t_{res}$  is the average residence time of all gases in the flow-tube (150 s). Detailed descriptions of a typical experiment can be found in Rutter et al. (2014), and all experiments described in this study follow the same procedures except the modifications mentioned below. Additional experimental information is provided in the Supporting material and Table S2.

Engine oil particles (100 nm, <150 #/cm<sup>3</sup>) were shown in Rutter et al. (2014) to have no effect on the reaction. During several tests, larger concentrations of motor oil particles were injected (up to 1400 #/cm<sup>3</sup>) into the mixture of VOCs and HNO<sub>3</sub>, and the particles had no observable impact on HONO levels. Therefore, for all experiments presented here motor oil particles were not considered relevant and were excluded by filtering the output from the atomizer upstream of the flow tube reactor. Fig. 1 depicts the experimental setup used in this study. A detailed diagram for the delivery of HNO<sub>3</sub> and VOCs can be found in Rutter et al. (2014).

Variations to the base case experiments were achieved by independently varying chamber temperature or HNO<sub>3</sub> concentration or by introducing UV irradiation, NH<sub>3</sub>, or mineral dust aerosol surrogate to the system. When a parameter was altered or a new constituent was added, all other base case variables remained unchanged. Apart from HNO<sub>3</sub> and NH<sub>3</sub> experiments discussed in sections 2.3 and 2.4, all experiments in this study were conducted

at initial HNO<sub>3</sub> concentrations of ~2–4 ppb for consistency with the experiments of Rutter et al. (2014) and the field measurements of Ziemba et al. (2010).

## 2.2. Temperature

This study aims to investigate the sensitivity of  $f_{HONO}$  to reaction temperature. Because the proposed reduction reaction of HNO<sub>3</sub> by VOCs may involve simultaneous reactions of different reactive VOCs of the engine oil blend, the temperature dependence of the overall formation rate is not expected to follow Arrhenius behavior. Investigation of temperature dependence is achieved by a temperature-controlled environmental test chamber (Espec North America Inc., Hudsonville, MI). The flow-tube and other components were allowed to equilibrate at the desired set-point temperature before an experiment. The measured reactor outflow temperatures were within ~1 °C of the set-point chamber temperatures. The temperature range tested here is relevant for the conditions observed in the 2006 Houston field study.

## 2.3. HNO<sub>3</sub> concentration

Initial HNO<sub>3</sub> mixing ratios were kept relatively constant in the experiments by Rutter et al. (2014), but minor fluctuations in HNO<sub>3</sub> between experiments were impossible to avoid. Nitric acid concentration was not considered important by Rutter et al. (2014) because the HNO<sub>3</sub> levels were in excess of the estimated 200–300 ppt reactive VOCs in the reactor. Here, experiments conducted at different initial concentrations of HNO<sub>3</sub> were used to probe this hypothesis and to investigate potential impacts of HNO<sub>3</sub> levels on the proposed reaction.

The steady-state HNO<sub>3</sub> concentrations in the flow-tube were varied in these experiments by operating the permeation device at different temperatures or by shutting off its supply entirely. Holding other parameters constant, HNO<sub>3</sub> mixing ratios of approximately 4.0 ppb, 1.5 ppb, and 0.4 ppb were achieved. The

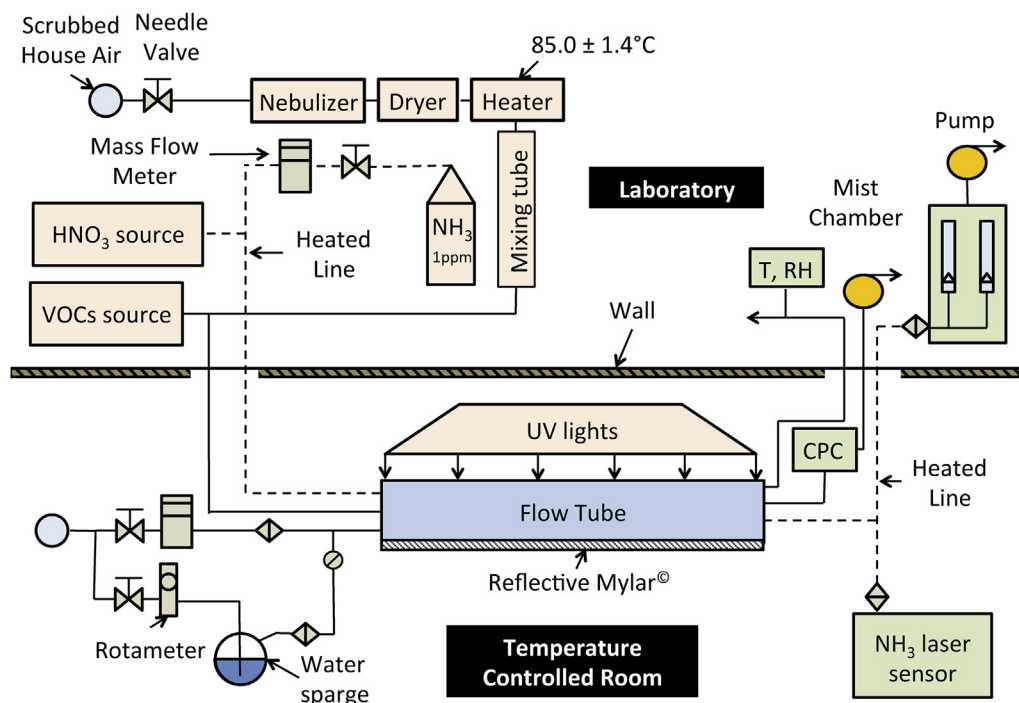


Fig. 1. Flow diagram of the flow-tube system and instrumentation. Dashed lines represent heated lines for the flow of low-volatility gases (CPC = condensation particle counter).

corresponding experiments are henceforth referred to as high  $\text{HNO}_3$ , medium  $\text{HNO}_3$ , and low  $\text{HNO}_3$  experiments.

#### 2.4. $\text{NH}_3$

Ammonia reacts with  $\text{HNO}_3$  to form ammonium nitrate ( $\text{NH}_4\text{NO}_3$ ), which transitions to the particulate phase when specific thermodynamic criteria are met. This reaction is hypothesized as a potential competing reaction and was studied in the flow-tube reactor by the addition of  $\text{NH}_3$ . Experiments were performed by injecting  $118.0 \pm 2.0$  ppb of gas-phase  $\text{NH}_3$  to the flow-tube reactor. A 1-ppm  $\text{NH}_3$  cylinder supplied the  $\text{NH}_3$  gas stream, which was diluted upon entering the reactor. Ammonia concentrations were monitored using a 10.4- $\mu\text{m}$  external cavity quantum cascade laser that has been well characterized and tested (Gong et al., 2011, 2013). The instrument has a detection limit of 0.7 ppb and an accuracy of 7%, with a maximum time-resolution of 1 s. Because the MC collection efficiencies for  $\text{HNO}_3$  and HONO already exceed 95% (Dibb et al., 1994),  $\text{NH}_3$  is not expected to cause interferences in  $\text{HNO}_3$  and HONO measurements. There was no evidence of artifacts from particulate  $\text{NH}_4\text{NO}_3$  because the MC/IC sample stream was filtered.

#### 2.5. UV irradiation

A HONO artifact at a forested field site correlated with UV intensity, possibly due to the photochemical conversion of  $\text{HNO}_3$  to HONO on the wall of a glass sampling manifold (Zhou et al., 2002). Laboratory experiments conducted by Zhou et al. (2003) found evidence that photolysis of adsorbed  $\text{HNO}_3$  on Pyrex surfaces yields HONO, and Zhou et al. (2011) found a significant HONO daytime source from the photolysis of  $\text{HNO}_3$  on forest canopies. These findings emphasize the potential role of UV irradiation in the conversion of  $\text{HNO}_3$  to HONO. Despite the observations of Rutter et al. (2014) and Ziemba et al. (2010) that light is not required for the proposed (R3) to proceed, it is hypothesized that UV irradiation may either accelerate (R3) or dampen it by consuming the reactive VOCs involved. Thus, experiments were conducted to test the sensitivity of  $f_{\text{HONO}}$  to UV irradiation.

Four 4-ft, 40 W Sylvania 350BL lights (Osram Sylvania, Danvers, MA) irradiated the flow-tube reactor for one set of experiments. Totalling 160 W of output, these tubes were mounted above the reactor and were distributed evenly along the length of the reactor. The reactor and lights were encased in Mylar reflective material to maximize light intensity and to ensure uniform distribution of the artificial light (peak  $\lambda = 350$  nm). The same type of lights was used in the chamber experiments of Cocker et al. (2001). This wavelength produces maximum  $\text{NO}_2$  photolysis rates (Carter et al., 1995) and falls within the UV-A spectrum (320–400 nm), which has been reported to photolyze species such as HONO (Stutz et al., 2000; Alicke et al., 2002). Thus, the lamps were considered a viable starting point to test for direct interferences on the hypothesized HONO formation reaction.

#### 2.6. Mineral dust aerosol surfaces

Field data collected in Houston during 2006 showed the potential for heterogeneous reduction of  $\text{HNO}_3$  into HONO on urban aerosol (Ziemba et al., 2010). However, Rutter et al. (2014) showed that the HONO formation reaction does not occur heterogeneously on engine oil particles or on a large surface area of Teflon<sup>®</sup> material. Grassian (2002) observed  $\text{HNO}_3$  heterogeneous uptake on mineral dust (alumina ( $\text{Al}_2\text{O}_3$ ) and silica ( $\text{SiO}_2$ )) surfaces and heterogeneous HONO production reactions from  $\text{NO}_2$  on soot or  $\text{SiO}_2$  particles. Gustafsson et al. (2008) observed heterogeneous production of HONO on mineral dust (from the Gobi desert) from  $\text{NO}_2$  and water.

Because mineral dust aerosols have more polar surfaces when compared to the engine oil and Teflon<sup>®</sup> surfaces, they are hypothesized to be better candidates for heterogeneous conversion of  $\text{HNO}_3$  to HONO. Two types of atmospherically abundant mineral dust materials were chosen for these experiments: carboxylate-doped  $\text{SiO}_2$  and  $\text{Al}_2\text{O}_3$ .

Aqueous dispersions of size-calibrated 100-nm monodisperse spherical particles composed of either carboxylated- $\text{SiO}_2$  or pure  $\text{Al}_2\text{O}_3$  (Corpuscular Inc., Cold Spring, NY) were used to generate aerosols for these experiments. These solutions were nebulized using an atomizer and subsequently dried using a diffusion-dryer and a heater ( $87.5 \pm 1.5$  °C).

### 3. Results and discussion

#### 3.1. Base case results

Compared with the previous flow-tube study, the average base case  $f_{\text{HONO}}$  of  $0.54 \pm 0.09$  ppb  $\text{h}^{-1}$  (Table 1) agrees better with the observed 2006 Houston value of  $0.6 \pm 0.3$  ppb  $\text{h}^{-1}$  (Ziemba et al., 2010; Rutter et al., 2014). This could be attributed to improved measurement accuracy due to the refurbished MC/IC system. This observation also suggests that the reduction of  $\text{HNO}_3$  to HONO by the reactive components of vehicular VOCs that were co-emitted with POA (Rutter et al., 2014) could be a dominant contributor to HONO formation events observed in Houston. The comparison here is qualitative because meteorology and vertical mixing conditions are highly variable in the atmosphere, and temperature ranged from 20.0 to 35.0 °C during this field campaign (Lefer et al., 2010). Additionally, it is worth noting that experiments conducted using pure VOCs (toluene, isoprene, and hexadecane) in place of motor oil VOCs did not result in net HONO production, ruling out these VOCs as potential reactants. These experiments also rule out HONO artifacts from reactions other than (R3). In other words, despite the <10%  $\text{HNO}_3$ -to-HONO conversion efficiency we generally observe in the flow-tube system (Rutter et al., 2014), other nitrogen-containing compounds originating from  $\text{HNO}_3$  reduction likely did not contribute to HONO production in this system.

Table 1 summarizes experimental data for each type of experiment. Mean values are reported for initial  $\text{HNO}_3$  concentrations,  $f_{\text{HONO}}$ , and water vapor mixing ratios with  $N \geq 3$ . All error bars and uncertainties reported here were propagated from measurement uncertainties, except those for initial  $\text{HNO}_3$  concentrations with  $N \geq 3$ , which are reported as standard deviations from the mean. The measurement uncertainties were larger than the standard deviations for  $f_{\text{HONO}}$  in most experiment types, indicating high repeatability. Additional information on uncertainty is included in the Supporting material.

The average HONO formation rates are not statistically different (within  $1\sigma$ ) when initial  $\text{HNO}_3$  concentrations were ~400, 1 500, and 4000 ppt, suggesting that the 200–300 ppt of reactive VOCs previously estimated by Rutter et al. (2014) (assuming a 1-to-1 stoichiometric ratio) remains the limiting factor. The lowest  $\text{HNO}_3$  concentrations achieved in these experiments were ~400 ppt (by shutting off  $\text{HNO}_3$  supply), which likely reflects the presence of  $\text{HNO}_3$  in the air source or the desorption of  $\text{HNO}_3$  from the supply tubing, since reactor walls were first rinsed with deionized water and baked under UV lights. A regression showing the weak relationship between  $f_{\text{HONO}}$  and  $\text{HNO}_3$  mixing ratio is shown in Fig. S1. Because  $\text{HNO}_3$  concentrations above 400 ppt do not appear to significantly impact  $f_{\text{HONO}}$ , all seven  $\text{HNO}_3$  experiments were grouped into one base case category (Table 1). This base case and the Houston 2006 average provide the benchmarks for comparison with other experiments (Fig. 2).

**Table 1**  
Summary of experimental conditions and average HONO formation rates.

Experiment	Initial HNO <sub>3</sub> (ppt)	Unc/stdev (ppt)	N <sup>a</sup>	<i>f</i> <sub>HONO</sub> (ppb/hr)	Unc/stdev (ppb/hr)	Water Vapor mixing ratio (%)	Notes
Base case, high HNO <sub>3</sub>	3980	936	3	0.60	0.16	0.67	T = 25.0 °C
Base case, medium HNO <sub>3</sub>	1522	159	3	0.51	0.08	0.63	T = 25.0 °C
Base case, low HNO <sub>3</sub>	399	53	1	0.43	0.25	0.58	T = 25.0 °C
Base case, all HNO <sub>3</sub> levels	2415	1613	7	0.54	0.09	0.64	T = 25.0 °C
T = 20.0 °C	2763	52	3	0.98	0.16	0.86	
T = 30.0 °C	4344	361	4	0.64	0.22	0.73	
T = 35.0 °C	3755	474	4	0.59	0.17	0.98	
UV irradiation	3405	451	3	0.37	0.17	0.59	Corrected for UV losses
Ammonia	680	52	3	0.60	0.11	0.73	NH <sub>3</sub> = 118.0 ± 2.0 ppb
Alumina aerosol	3356	346	3	0.45	0.07	0.61	Average count = 1600#/cm <sup>3</sup>
Silica-COOH aerosol	3443	85	3	0.43	0.10	0.60	Average count = 1600#/cm <sup>3</sup>

<sup>a</sup> N = number of experiments conducted.

### 3.2. Temperature

Although the mean *f*<sub>HONO</sub> value for the combined base case experiments (T = 25 °C) was lower than that for other temperatures, the *f*<sub>HONO</sub> at 30.0 °C and 35.0 °C are not statistically different (within 1σ) than that of the base case. However, experiments at 20.0 °C yielded significantly higher *f*<sub>HONO</sub> (above 1σ). This could mean that the reaction rate increases at lower temperatures, but as mentioned previously this dependence may not follow an Arrhenius trend. This trend suggests the possibility that multiple reactions involving different reactive VOCs become more important at various temperatures. Sampling lines were insulated and heated such that HONO wall losses would be as small as possible, but it should be noted that any bias due to wall losses would likely decrease *f*<sub>HONO</sub> at lower temperatures. The enhanced rate at lower temperatures could make the proposed reaction mechanism even more important at night.

### 3.3. NH<sub>3</sub>

The presence of NH<sub>3</sub> had no observable impact on the reaction. Nitric acid concentrations were at ~3500 ppt before NH<sub>3</sub> was introduced. After addition of NH<sub>3</sub>, the system equilibrated at

118.0 ± 2.0 ppb NH<sub>3</sub> and 680 ± 52 ppt HNO<sub>3</sub>. The formation of NH<sub>4</sub>NO<sub>3</sub> and its subsequent partitioning into the solid phase is the likely cause for the observed consumption of HNO<sub>3</sub>; any NH<sub>4</sub>NO<sub>3</sub> particles formed would be filtered prior to entering the MC/IC. The *f*<sub>HONO</sub> for these experiments also were similar to the base case, likely because HNO<sub>3</sub> was still in excess compared to the VOCs. This indicates that the neutralization reaction between NH<sub>3</sub> and HNO<sub>3</sub> does not directly interfere with the HONO formation reaction beyond the competition for HNO<sub>3</sub>. Consistent with the experiments under varying HNO<sub>3</sub> levels, a lower *f*<sub>HONO</sub> is not observed due to the decrease in HNO<sub>3</sub>.

### 3.4. UV light

When UV lights were turned on prior to experiments, a constant photolytic source of HONO from HNO<sub>3</sub> was observed, contributing to background HONO levels (net production of ~226 ppt or ~5.42 ppb h<sup>-1</sup>) in the reactor. Several sources could explain this HONO production, for example direct photolysis of HNO<sub>3</sub> sorbed on the reactor walls (Zhou et al., 2003) or from photolysis of nitrophenols (Bejan et al., 2006) that could be present in lubricating oil. We do not have the capability to isolate these sources, but they are not expected to bias *f*<sub>HONO</sub> as defined here because formation rates are calculated using a step change in HONO when VOCs were removed during an experiment (Equation (1)). In other words, the HONO formation observed when VOCs were introduced under UV irradiation occurs above and beyond the background photolytic sources.

The observed average *f*<sub>HONO,obs</sub> under UV irradiation of 0.29 ± 0.17 ppb h<sup>-1</sup> was obtained using the change in HONO levels when VOCs were removed, similar to other experiments. However, according to a simplified mass balance (Equation (2)), the actual HONO production rate (*f*<sub>HONO,UV</sub>) must correct for photolytic losses of HONO generated when VOCs were present to react with HNO<sub>3</sub>:

$$f_{HONO,UV} = f_{HONO,obs} + J_{HONO}([HONO]_{UV+VOCs} - [HONO]_{UV}) \quad (2)$$

where *J*<sub>HONO</sub> is the photolysis rate of HONO, and the term in brackets represents the difference in measured HONO mixing ratios with and without VOCs when the lights are illuminated. A spectroradiometer was not available to determine *J*<sub>HONO</sub>. In Equation (2), an average *J*<sub>HONO</sub> value of 1.75 × 10<sup>-3</sup> s<sup>-1</sup> was used. This value was derived from an average of measured ambient noon-time *J*<sub>HONO</sub> (1.75 × 10<sup>-3</sup> s<sup>-1</sup> (Alicke et al., 2003) and 1.60 × 10<sup>-3</sup> s<sup>-1</sup> (Lee et al., 2013)) and *J*<sub>HONO</sub> estimated using the method from Kraus and Hofzumahaus (1998) (1.90 × 10<sup>-3</sup> s<sup>-1</sup>) from NO<sub>2</sub> photolysis rates reported in an environmental chamber (Nakao et al., 2011) that utilized the same model of lights as this study. When corrected, the average *f*<sub>HONO,UV</sub> is 0.37 ± 0.17 ppb h<sup>-1</sup> (Table 1 and Fig. 2).

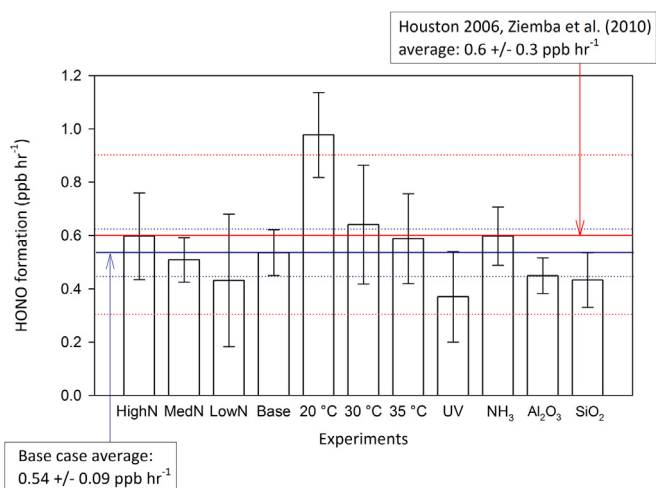


**Fig. 2.** Average HONO formation rates (with error bars) for each experimental category and comparison to the base case (25.0 °C and ~20.0% RH without the addition of NH<sub>3</sub>, dust particles, or UV irradiation) and field results from Ziemba et al. (2010). Dotted lines indicate 1σ bands for the base case and field results. HighN, MedN, and LowN represent experiments with high HNO<sub>3</sub>, medium HNO<sub>3</sub>, and low HNO<sub>3</sub>, respectively, and are combined to generate the average base case output. The average HONO formation rate for UV experiments was corrected for photolytic HONO losses (see Section 3.4).

However, the  $J_{\text{HONO}}$  used here is likely much higher than the actual value from only four 40 W UV lights, indicating that the  $f_{\text{HONO, UV}}$  is likely an upper bound. To further test the uncertainty, the estimated value of  $J_{\text{HONO}}$  used was adjusted by factors of 0.5 and 2 to provide a range of  $0.33 \pm 0.17$  to  $0.44 \pm 0.17$  ppb  $\text{h}^{-1}$  for the potential average  $f_{\text{HONO, UV}}$  values.

Although  $f_{\text{HONO, UV}}$  is within the uncertainty range of the base case  $f_{\text{HONO}}$ , it is likely that the reported  $f_{\text{HONO, UV}}$  represents an upper bound and that the UV wavelengths studied here could directly interfere with the reduction reaction of  $\text{HNO}_3$  to HONO. One explanation for this observation is that under UV irradiation, relevant organic compounds undergo oxidation by radicals formed in the reactor (Atkinson, 2000) or are photolyzed directly. This could alter the reactivity of the VOCs or reduce the total concentration of reactive VOCs available for reaction, hence slowing the overall reaction rate. This and additional tests (Support Material) support the hypothesis that VOCs are the limiting reactants in the reaction proposed here.

### 3.5. Mineral dust aerosol surfaces

Neither carboxylated- $\text{SiO}_2$  nor  $\text{Al}_2\text{O}_3$  particles (at concentrations of  $\sim 1600$   $\#/\text{cm}^3$ ) yielded significantly different  $f_{\text{HONO}}$  (within 1 $\sigma$ ) than the base case (Fig. 2). The slight decrease observed is counterintuitive if the surfaces are expected to enhance the reaction, indicating that the surfaces are potential minor loss sites for the reactive VOCs involved or for the HONO produced (Romanias et al., 2012). This further affirms the probability that a surface is not required to convert  $\text{HNO}_3$  to HONO via the proposed pathway.

## 4. Conclusions

Estimates of base case (25 °C,  $\sim 20\%$  RH)  $f_{\text{HONO}}$  derived from the reduction of  $\text{HNO}_3$  by VOCs agree well with data from a 2006 field study in Houston (Ziemba et al., 2010) during which enhancements in HONO during morning rush hour were observed. The hypothesized reaction (R3) studied here could have been the main HONO source during the HONO formation events.

The HONO formation rate was relatively enhanced ( $\sim 1.0$  ppb  $\text{h}^{-1}$ ) at a lower temperature of  $\sim 20$  °C but statistically the same ( $\sim 0.6$  ppb  $\text{h}^{-1}$ ) in experiments at 25, 30 and 35 °C. The assumption that multiple reactive components of the VOCs react with  $\text{HNO}_3$  is supported by this observation, and the relative importance of each reactive species in the reaction may vary with temperature. The reaction rate is independent of initial  $\text{HNO}_3$  concentration ( $>400$  ppt), suggesting that the concentration of reactive VOCs was the limiting factor. However, future work testing this reaction under  $\text{HNO}_3$  concentrations  $<400$  ppt may provide insights into its relevance in cleaner environments. Ammonia gas consumed  $\text{HNO}_3$  in the reactor (down to 680 ppt) but did not have a direct impact on the HONO formation reaction, providing further evidence that the rate is limited by the availability of VOCs in the experimental system. The  $f_{\text{HONO, UV}}$  from (R3) was likely impeded by UV irradiation. Possible explanations for this observation include the photolysis/deactivation of the reactive VOCs involved in (R3) or the direct interference of UV light on (R3). Nonetheless, this observation must be confirmed by conducting a similar flow-tube study that focuses on constraining the reactive VOCs involved and quantifying HONO photolysis rates. The test of multiple atmospherically-relevant particle surfaces confirmed that the reaction proposed here does not require surfaces to proceed, despite the correlation that was observed in Houston in 2006 (Ziemba et al., 2010). Given the uncertainties, we observe substantial percentage changes in  $f_{\text{HONO}}$  between the base case and the 20 °C and UV experiments, even when compared to the change when RH was varied from the base case to 1% or 50% in Rutter et al. (2014). The

reduced sensitivity of  $f_{\text{HONO}}$  to other environmental variables tested here is also an important finding, especially in future modeling work aiming at incorporating this new HONO source to existing atmospheric models.

The HONO formation process studied here is likely homogeneous, but the results presented here do not rule out the possibility of a heterogeneous reaction pathway occurring in the atmosphere. Also, it is important to note that the net production of HONO observed in the UV experiments is in addition to production by background photolytic reactions that appear to be occurring on the wax-coated tube walls.

The gas-phase conversion of  $\text{HNO}_3$  to HONO has significant air quality implications due to the “renoxification” of less reactive  $\text{HNO}_3$  into more reactive HONO and should be tested in future modeling and field efforts. This pathway proceeds rapidly in the laboratory when compared with previously identified mechanisms (Table S3) and could potentially be an important source of HONO in the lower atmosphere (2nd order rate constant  $\sim 1.0 \times 10^{-7}$  ppt $^{-1}$  s $^{-1}$  estimated in Gall et al. (2016), in revision for *Atmospheric Environment*). Its role in HONO production aloft (synonymous to the unknown gas-phase HONO source proposed by Li et al. (2014)) cannot yet be ruled out and should be evaluated in future work. In addition to their direct impact on  $\text{O}_3$  formation and secondary organic aerosol formation, VOCs could also regulate the oxidative capacity of the atmosphere through the redox reaction studied here. These different processes have significant implications in terms of regional and global air quality. Hence, future experimental work focusing on the quantification of individual reactive components of the VOCs (e.g. utilizing mass spectrometry techniques coupled with proton transfer reaction or gas chromatography) that were involved in the reaction studied here (under varying environmental conditions) would allow detailed characterization of the HONO formation mechanism(s) and determination of reaction yields. Once the HONO formation reaction mechanism is well characterized, parameterizing the reaction would allow improvements in existing  $\text{O}_3$  and PM prediction models.

## Conflict of interest

The authors of this study do not have any personal/financial conflicts of interest that could interfere with the objectivity of this work.

## Acknowledgments

We acknowledge financial support from the National Aeronautics and Space Administration (NASA Grant #NNX09AE26G S04). Ammonia measurements were supported by the National Science Foundation through the Mid-InfraRed Technologies for Health and the Environment (MIRTHE) Center under grant No. EEC-0540832; Dan Campbell assisted in the ammonia experiments.

## Appendix A. Supplementary data

Supplementary data related to this article can be found at <http://dx.doi.org/10.1016/j.apr.2015.09.006>.

## References

- Alicke, B., Geyer, A., Hofzumahaus, A., Holland, F., Konrad, S., Pätz, H.W., Schäfer, J., Stutz, J., Volz-Thomas, A., Platt, U., 2003. OH formation by HONO photolysis during the BERLIOZ experiment. *J. Geophys. Res. Atmos.* 108, 8247. <http://dx.doi.org/10.1029/2001JD000579>.
- Alicke, B., Platt, U., Stutz, J., 2002. Impact of nitrous acid photolysis on the total hydroxyl radical budget during the limitation of oxidant production/Pianura Padana Produzione di Ozono study in Milan. *J. Geophys. Res. Atmos.* 107, 8196. <http://dx.doi.org/10.1029/2000JD000075>.

- Ammann, M., Kalberer, M., Jost, D.T., Tobler, L., Rossler, E., Piguet, D., Gaggeler, H.W., Baltensperger, U., 1998. Heterogeneous production of nitrous acid on soot in polluted air masses. *Nature* 395, 157–160. <http://dx.doi.org/10.1038/25965>.
- Atkinson, R., 2000. Atmospheric chemistry of VOCs and NO<sub>x</sub>. *Atmos. Environ.* 34, 2063–2101. [http://dx.doi.org/10.1016/S1352-2310\(99\)00460-4](http://dx.doi.org/10.1016/S1352-2310(99)00460-4).
- Bejan, I., Abd El Aal, Y., Barnes, I., Benter, T., Bohn, B., Wiesen, P., Kleffmann, J., 2006. The photolysis of ortho-nitrophenols: a new gas phase source of HONO. *Phys. Chem. Chem. Phys.* 8, 2028–2035. <http://dx.doi.org/10.1039/B516590C>.
- Cape, J.N., Hargreaves, K.J., Storeton-West, R., Fowler, D., Colville, R.N., Choulaton, T.W., Gallagher, M.W., 1992. Nitrite in orographic cloud as an indicator of nitrous acid in rural air. *Atmos. Environ. Part A. General Top.* 26, 2301–2307. [http://dx.doi.org/10.1016/0960-1686\(92\)90361-N](http://dx.doi.org/10.1016/0960-1686(92)90361-N).
- Carter, W.P.L., Luo, D., Malkina, I.L., Pierce, J.A., 1995. *Environmental Chamber Studies of Atmospheric Reactivities of Volatile Organic Compounds. Effects of Varying Chamber and Light Source. Final report. University of California, Riverside*.
- Carter, W.P.L., Seinfeld, J.H., 2012. Winter ozone formation and VOC incremental reactivities in the Upper Green River Basin of Wyoming. *Atmos. Environ.* 50, 255–266. <http://dx.doi.org/10.1016/j.atmosenv.2011.12.025>.
- Cazoir, D., Brigante, M., Ammar, R., D'Anna, B., George, C., 2014. Heterogeneous photochemistry of gaseous NO<sub>2</sub> on solid fluoranthene films: a source of gaseous nitrous acid (HONO) in the urban environment. *J. Photochem. Photobiol. a-Chem.* 273, 23–28. <http://dx.doi.org/10.1016/j.jphotochem.2013.07.016>.
- Cocker, D.R., Flagan, R.C., Seinfeld, J.H., 2001. State-of-the-art chamber facility for studying atmospheric aerosol chemistry. *Environ. Sci. Technol.* 35, 2594–2601. <http://dx.doi.org/10.1021/es0019169>.
- Dibb, J.E., Arsenaault, M., Peterson, M.C., Honrath, R.E., 2002. Fast nitrogen oxide photochemistry in Summit, Greenland snow. *Atmos. Environ.* 36, 2501–2511. [http://dx.doi.org/10.1016/S1352-2310\(02\)00130-9](http://dx.doi.org/10.1016/S1352-2310(02)00130-9).
- Dibb, J.E., Talbot, R.W., Bergin, M.H., 1994. Soluble acidic species in air and snow at Summit, Greenland. *Geophys. Res. Lett.* 21, 1627–1630. <http://dx.doi.org/10.1029/94gl01031>.
- Dibb, J.E., Talbot, R.W., Munger, J.W., Jacob, D.J., Fan, S.M., 1998. Air-snow exchange of HNO<sub>3</sub> and NO<sub>y</sub> at Summit, Greenland. *J. Geophys. Research-Atmos.* 103, 3475–3486. <http://dx.doi.org/10.1029/97jd03132>.
- Finlayson-Pitts, B.J., Pitts, J.N., 1997. Tropospheric air pollution: ozone, airborne toxics, polycyclic aromatic hydrocarbons, and particles. *Science* 276, 1045–1052. <http://dx.doi.org/10.1126/science.276.5315.1045>.
- Gall, E.T., Dibb, J., Scheuer, E., Gong, L., Rutter, A.P., Karakurt Cevik, B., Kim, S., Lefer, B., Flynn, J., Griffin, R.J., 2016. Nitrous acid formation mechanisms in the outflow from a major urban area. *Atmos. Environ.* <http://dx.doi.org/10.1016/j.atmosenv.2015.12.044>.
- Gong, L., Lewicki, R., Griffin, R.J., Flynn, J.H., Lefer, B.L., Tittel, F.K., 2011. Atmospheric ammonia measurements in Houston, TX using an external-cavity quantum cascade laser-based sensor. *Atmos. Chem. Phys.* 11, 9721–9733. <http://dx.doi.org/10.5194/acp-11-9721-2011>.
- Gong, L., Lewicki, R., Griffin, R.J., Tittel, F.K., Lonsdale, C.R., Stevens, R.G., Pierce, J.R., Malloy, Q.G.J., Travis, S.A., Bobmanuel, L.M., Lefer, B.L., Flynn, J.H., 2013. Role of atmospheric ammonia in particulate matter formation in Houston during summertime. *Atmos. Environ.* 77, 893–900. <http://dx.doi.org/10.1016/j.atmosenv.2013.04.079>.
- Grannas, A.M., Jones, A.E., Dibb, J., Ammann, M., Anastasio, C., Beine, H.J., Bergin, M., Bottenheim, J., Boxe, C.S., Carver, G., Chen, G., Crawford, J.H., Dominé, F., Frey, M.M., Guzmán, M.J., Heard, D.E., Helmig, D., Hoffmann, M.R., Honrath, R.E., Huey, L.G., Hutterli, M., Jacobi, H.W., Klán, P., Lefer, B., McConnell, J., Plane, J., Sander, R., Savarino, J., Shepson, P.B., Simpson, W.R., Sodeau, J.R., von Glasow, R., Weller, R., Wolff, E.W., Zhu, T., 2007. An overview of snow photochemistry: evidence, mechanisms and impacts. *Atmos. Chem. Phys.* 7, 4329–4373. <http://dx.doi.org/10.5194/acp-7-4329-2007>.
- Grassian, V.H., 2002. Chemical reactions of nitrogen oxides on the surface of oxide, carbonate, soot, and mineral dust particles: Implications for the chemical balance of the troposphere. *J. Phys. Chem. A* 106, 860–877. <http://dx.doi.org/10.1021/jp012139h>.
- Gustafsson, R.J., Kyriakou, G., Lambert, R.M., 2008. The molecular mechanism of tropospheric nitrous acid production on mineral dust surfaces. *ChemPhysChem* 9, 1390–1393. <http://dx.doi.org/10.1002/cphc.200800259>.
- Harris, G.W., Carter, W.P.L., Winer, A.M., Pitts, J.N., Platt, U., Perner, D., 1982. Observations of nitrous acid in the Los Angeles atmosphere and implications for predictions of ozone-precursor relationships. *Environ. Sci. Technol.* 16, 414–419. <http://dx.doi.org/10.1021/es00101a009>.
- Harrison, R.M., Peak, J.D., Collins, G.M., 1996. Tropospheric cycle of nitrous acid. *J. Geophys. Res. Atmos.* 101, 14429–14439. <http://dx.doi.org/10.1029/96JD00341>.
- Indarto, A., 2012. Heterogeneous reactions of HONO formation from NO<sub>2</sub> and HNO<sub>3</sub>: a review. *Res. Chem. Intermed.* 38, 1029–1041. <http://dx.doi.org/10.1007/s11164-011-0439-z>.
- Kalberer, M., Ammann, M., Arens, F., Gaggeler, H.W., Baltensperger, U., 1999. Heterogeneous formation of nitrous acid (HONO) on soot aerosol particles. *J. Geophys. Research-Atmos.* 104, 13825–13832. <http://dx.doi.org/10.1029/1999jd900141>.
- Kanakidou, M., Seinfeld, J.H., Pandis, S.N., Barnes, I., Dentener, F.J., Facchini, M.C., Van Dingenen, R., Ervens, B., Nenes, A., Nielsen, C.J., Swietlicki, E., Putaud, J.P., Balkanski, Y., Fuzzi, S., Horth, J., Moortgat, G.K., Winterhalter, R., Myhre, C.E.L., Tsigaridis, K., Vignati, E., Stephanou, E.G., Wilson, J., 2005. Organic aerosol and global climate modelling: a review. *Atmos. Chem. Phys.* 5, 1053–1123.
- Kirchstetter, T.W., Harley, R.A., Littlejohn, D., 1996. Measurement of nitrous acid in motor vehicle exhaust. *Environ. Sci. Technol.* 30, 2843–2849. <http://dx.doi.org/10.1021/es960135y>.
- Kleffmann, J., 2007. Daytime sources of nitrous acid (HONO) in the atmospheric boundary layer. *ChemPhysChem* 8, 1137–1144. <http://dx.doi.org/10.1002/cphc.200700016>.
- Kraus, A., Hofzumahaus, A., 1998. Field measurements of atmospheric photolysis frequencies for O-3, NO<sub>2</sub>, HCHO, CH<sub>3</sub>CHO, H<sub>2</sub>O<sub>2</sub>, and HONO by UV spectroradiometry. *J. Atmos. Chem.* 31, 161–180. <http://dx.doi.org/10.1023/a:1005888220949>.
- Lee, B.H., Wood, E.C., Herndon, S.C., Lefer, B.L., Luke, W.T., Brune, W.H., Nelson, D.D., Zahniser, M.S., Munger, J.W., 2013. Urban measurements of atmospheric nitrous acid: a caveat on the interpretation of the HONO photostationary state. *J. Geophys. Res. Atmos.* 118, 12274–12281. <http://dx.doi.org/10.1002/2013JD020341>.
- Lefer, B., Rappenglück, B., Flynn, J., Haman, C., 2010. Photochemical and meteorological relationships during the Texas-II Radical and Aerosol Measurement Project (TRAMP). *Atmos. Environ.* 44, 4005–4013. <http://dx.doi.org/10.1016/j.atmosenv.2010.03.011>.
- Lei, W., Zhang, R., Tie, X., Hess, P., 2004. Chemical characterization of ozone formation in the Houston-Galveston area: a chemical transport model study. *J. Geophys. Res. Atmos.* 109, D12301. <http://dx.doi.org/10.1029/2003JD004219>.
- Li, X., Rohrer, F., Hofzumahaus, A., Brauers, T., Haseler, R., Bohn, B., Broch, S., Fuchs, H., Gomm, S., Holland, F., Jäger, J., Kaiser, J., Keutsch, F.N., Lohse, I., Lu, K.D., Tillmann, R., Wegener, R., Wolfe, G.M., Mentel, T.F., Kändler-Scharr, A., Wahner, A., 2014. Missing gas-phase source of HONO inferred from zeppelin measurements in the troposphere. *Science* 344, 292–296. <http://dx.doi.org/10.1126/science.1248999>.
- Liu, Z., Wang, Y., Costabile, F., Amoroso, A., Zhao, C., Huey, L.G., Stickel, R., Liao, J., Zhu, T., 2014. Evidence of aerosols as a media for rapid daytime HONO production over China. *Environ. Sci. Technol.* 48, 14386–14391. <http://dx.doi.org/10.1021/es504163z>.
- Nakao, S., Shrivastava, M., Nguyen, A., Jung, H.J., Cocker, D., 2011. Interpretation of secondary organic aerosol formation from diesel exhaust photooxidation in an environmental chamber. *Aerosol Sci. Technol.* 45, 9. <http://dx.doi.org/10.1080/02786826.2011.573510>.
- Reisinger, A.R., 2000. Observations of HNO<sub>2</sub> in the polluted winter atmosphere: possible heterogeneous production on aerosols. *Atmos. Environ.* 34, 3865–3874. [http://dx.doi.org/10.1016/S1352-2310\(00\)00179-5](http://dx.doi.org/10.1016/S1352-2310(00)00179-5).
- Rivera-Figueroa, A.M., Sumner, A.L., Finlayson-Pitts, B.J., 2003. Laboratory studies of potential mechanisms of renoxification of tropospheric nitric acid. *Environ. Sci. Technol.* 37, 548–554. <http://dx.doi.org/10.1021/es020828g>.
- Romanias, M.N., El Zein, A., Bedjanian, Y., 2012. Reactive uptake of HONO on aluminium oxide surface. *J. Photochem. Photobiol. a-Chem.* 250, 50–57. <http://dx.doi.org/10.1016/j.jphotochem.2012.09.018>.
- Rutter, A.P., Malloy, Q.G.J., Leong, Y.J., Gutierrez, C.V., Calzada, M., Scheuer, E., Dibb, J.E., Griffin, R.J., 2014. The reduction of HNO<sub>3</sub> by volatile organic compounds emitted by motor vehicles. *Atmos. Environ.* 87, 200–206. <http://dx.doi.org/10.1016/j.atmosenv.2014.01.056>.
- Spataro, F., Ianniello, A., 2014. Sources of atmospheric nitrous acid: state of the science, current research needs, and future prospects. *J. Air Waste Manag. Assoc.* 64, 1232–1250. <http://dx.doi.org/10.1080/10962247.2014.952846>.
- Stutz, J., Kim, E.S., Platt, U., Bruno, P., Perrino, C., Febo, A., 2000. UV-visible absorption cross sections of nitrous acid. *J. Geophys. Research-Atmos.* 105, 14585–14592. <http://dx.doi.org/10.1029/2000jd900003>.
- Stutz, J., Oh, H.-J., Whitlow, S.I., Anderson, C., Dibb, J.E., Flynn, J.H., Rappenglück, B., Lefer, B., 2010. Simultaneous DOAS and mist-chamber IC measurements of HONO in Houston, TX. *Atmos. Environ.* 44, 4090–4098. <http://dx.doi.org/10.1016/j.atmosenv.2009.02.003>.
- Talbot, R.W., Vijgen, A.S., Harris, R.C., 1990. Measuring tropospheric HNO<sub>3</sub> - problems and prospects for nylon filter and mist chamber techniques. *J. Geophys. Research-Atmos.* 95, 7553–7561. <http://dx.doi.org/10.1029/JD095iD06p07553>.
- VandenBoer, T.C., Young, C.J., Talukdar, R.K., Markovic, M.Z., Brown, S.S., Roberts, J.M., Murphy, J.G., 2015. Nocturnal loss and daytime source of nitrous acid through reactive uptake and displacement. *Nat. Geosci.* 8, 55–60. <http://dx.doi.org/10.1038/ngeo2298>.
- Wong, K.W., Oh, H.J., Lefer, B.L., Rappenglueck, B., Stutz, J., 2011. Vertical profiles of nitrous acid in the nocturnal urban atmosphere of Houston, TX. *Atmos. Chem. Phys.* 11, 3595–3609. <http://dx.doi.org/10.5194/acp-11-3595-2011>.
- Worton, D.R., Isaacman, G., Gentner, D.R., Dallmann, T.R., Chan, A.W.H., Ruehl, C., Kirchstetter, T.W., Wilson, K.R., Harley, R.A., Goldstein, A.H., 2014. Lubricating oil dominates primary organic aerosol emissions from motor vehicles. *Environ. Sci. Technol.* 48, 3698–3706. <http://dx.doi.org/10.1021/es405375j>.
- Zhou, X.L., Gao, H.L., He, Y., Huang, G., Bertman, S.B., Civerolo, K., Schwab, J., 2003. Nitric acid photolysis on surfaces in low-NO<sub>x</sub> environments: significant atmospheric implications. *Geophys. Res. Lett.* 30, 2217. <http://dx.doi.org/10.1029/2003gl018620>.
- Zhou, X.L., He, Y., Huang, G., Thornberry, T.D., Carroll, M.A., Bertman, S.B., 2002. Photochemical production of nitrous acid on glass sample manifold surface. *Geophys. Res. Lett.* 29 (4) <http://dx.doi.org/10.1029/2002gl015080>.
- Zhou, X.L., Zhang, N., TerAvest, M., Tang, D., Hou, J., Bertman, S., Alaghmand, M., Shepson, P.B., Carroll, M.A., Griffith, S., Dusanter, S., Stevens, P.S., 2011. Nitric acid photolysis on forest canopy surface as a source for tropospheric nitrous acid. *Nat. Geosci.* 4, 440–443. <http://dx.doi.org/10.1038/ngeo1164>.
- Ziamba, L.D., Dibb, J.E., Griffin, R.J., Anderson, C.H., Whitlow, S.I., Lefer, B.L., Rappenglück, B., Flynn, J., 2010. Heterogeneous conversion of nitric acid to nitrous acid on the surface of primary organic aerosol in an urban atmosphere. *Atmos. Environ.* 44, 4081–4089. <http://dx.doi.org/10.1016/j.atmosenv.2008.12.024>.